

On-demand single-electron transfer between distant quantum dots

R. P. G. McNeil¹, M. Kataoka^{1,2}, C. J. B. Ford¹, C. H. W. Barnes¹, D. Anderson¹, G. A. C. Jones¹, I. Farrer¹ & D. A. Ritchie¹

Single-electron circuits of the future, consisting of a network of quantum dots, will require a mechanism to transport electrons from one functional part of the circuit to another. For example, in a quantum computer¹ decoherence and circuit complexity can be reduced by separating quantum bit (qubit) manipulation from measurement and by providing a means of transporting electrons between the corresponding parts of the circuit². Highly controlled tunnelling between neighbouring dots has been demonstrated^{3,4}, and our ability to manipulate electrons in single- and double-dot systems is improving rapidly^{5–8}. For distances greater than a few hundred nanometres, neither free propagation nor tunnelling is viable while maintaining confinement of single electrons. **Here we show how a single electron may be captured in a surface acoustic wave minimum and transferred from one quantum dot to a second, unoccupied, dot along a long, empty channel.** The transfer direction may be reversed and the same electron moved back and forth more than sixty times—a cumulative distance of 0.25 mm—without error. Such on-chip transfer extends communication between quantum dots to a range that may allow the integration of discrete quantum information processing components and devices.

Our device consists of two quantum dots connected by a long channel (Fig. 1A). Negative voltages applied to patterned metal surface gates deplete a two-dimensional electron gas that lies 90 nm below the

surface. The voltages are chosen such that the potential of the system is above the Fermi energy, and in thermal equilibrium the dots and channel contain no electrons.

The quantum dots are adjusted by the two plunger and barrier gates. Each plunger raises and lowers the corresponding dot and each barrier controls the degree of isolation between that dot and the neighbouring reservoir. Charge in each quantum dot is detected by its effect on the conductance of high-resistance constrictions⁹ on the other side of a narrow ‘separation’ gate. A single electron can be initialized in one quantum dot (Fig. 1B, d) and then transferred at will to the other dot using a short burst of surface acoustic waves (SAWs). In a piezoelectric material (such as GaAs), SAWs create a moving potential modulation that can trap and transport electrons. The transferred electron can be returned using a second SAW pulse travelling in the opposite direction, giving two-way transfer.

Initialization of the dots is shown schematically in Fig. 1B. To set up an occupied left-hand quantum dot (LQD), the left-hand barrier gate (LBG) and left-hand plunger gate (LPG) are lowered to populate the LQD (Fig. 1B, a); the LBG is raised, isolating the LQD from the reservoir (Fig. 1B, b); and the LPG is raised to depopulate the dot selectively, leaving one electron (Fig. 1B, c) or more if desired (Supplementary Fig. 1). The LBG and LPG can then be stepped to their final voltages (Fig. 1B, d). The dot now contains a chosen number of electrons held close to, but below, the channel potential. An empty dot is initialized in

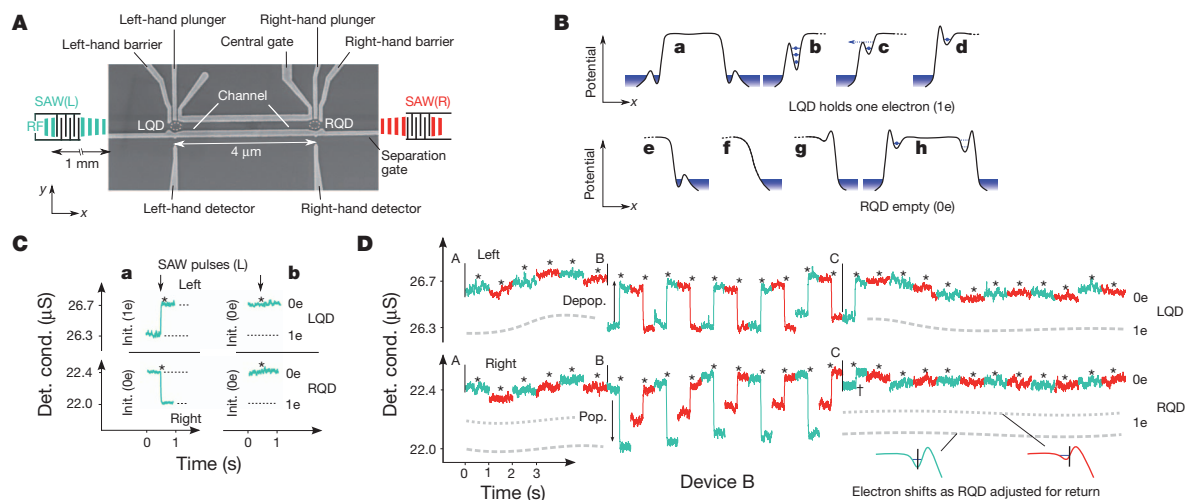


Figure 1 | Device, initialization and single-electron transfer. **A**, Scanning electron micrograph of device. Voltages applied to gates (light grey) create quantum dots (dashed circles) connected by a 4-μm channel. Applying a microwave (RF) pulse to the left- and right-hand transducers (placed 1 mm from the device) generates SAW pulses that trap and transport electrons. **B**, Schematic of the potential between the LQD and the RQD during initialization of the LQD with one electron (1e) (a–d) and then the RQD with no electrons (0e) (e–h). **C**, Change in detector conductance when SAW pulse (*) is applied to the system set up as in **B**, h. The empty RQD is populated when

the electron leaves the LQD. The second pair of traces shows a control case in which the LQD starts empty (0e) (traces are 1 s long). **D**, Single-electron rally: the quantum dots and the channel are initialized to be empty before time A. Between time A and time B, a series of control pulses is used to verify that system is empty. At time B an electron is loaded into LQD. Between time B and time C, there is two-way transfer of a single electron between the quantum dots. At time C, the electron is removed from the system using a clearing pulse. The SAW pulse duration is 300 ns. The small step marked ‘†’ is a random switching event and is not SAW driven. The time between traces is not plotted.

¹Cavendish Laboratory, University of Cambridge, J. J. Thomson Avenue, Cambridge CB3 0HE, UK. ²National Physical Laboratory, Hampton Road, Teddington TW11 0LW, UK.

a similar way but with the plunger gate being raised first (Fig. 1B, e–h). The final voltages for both the empty and occupied quantum dots (Fig. 1B, d and h) are the same and, thus, detector conductance indicates the number of electrons in each dot (Supplementary Information).

On-demand depopulation of an initialized quantum dot is achieved by a brief SAW pulse. Applying a microwave signal to the left-hand transducer generates a SAW. The accompanying potential modulation, moving at $2,870 \text{ m s}^{-1}$, captures the electron from the LQD and transfers it in 1.4 ns to the right-hand quantum dot (RQD). Part a of Fig. 1C shows the conductance of the left- and right-hand detectors for an occupied LQD (1e) and an unoccupied RQD (0e) when a SAW pulse (300 ns long) is sent from the left (SAW(L)). The transfer of charge is shown by simultaneous step changes in the detector conductance.

We know that the quantum dots are not simply exchanging electrons with their neighbouring reservoirs (in the direction opposite to that of SAW propagation) during the SAW pulse sequences, because in the control case, with an empty starting dot, no change in detector conductance is seen (Fig. 1C, b)). It is possible that electrons are instead being transferred by means of a ‘Newton’s cradle’ arrangement, whereby an electron from one dot moves into the channel, causing a series of electrons in traps along the channel to ‘shuffle up’, ejecting the last electron into the second dot. However, the SAW amplitude is 2.5 times greater than that at which electrons are caught in the channel, so there are no electrons to be shuffled along. Thus, in part a of Fig. 1C a single electron is being transferred between the dots.

The two transducers allow for bidirectional transfer between the quantum dots, and single electrons (or pairs) can be sent backwards and forwards in bursts (as in a game of ‘ping-pong’) with ‘rallies’ comprising tens to hundreds of SAW pulses. Figure 1D is an example of such a single-electron rally. Both quantum dots are emptied before time A, and six control pulses (three SAW(L)–SAW(R) pairs) show the system to be empty. At time B, an electron is loaded into the LQD. The electron is then sent back and forth by ten alternating SAW pulses (five pairs) until at time C the RQD barrier is partly lowered and a ‘clearing’ pulse removes the electron from the channel—in this case to the right-hand reservoir but potentially into the next section of a quantum dot circuit. The small step in the right detector signal (\dagger) is a random switching event near the detector. It is not coincident with the SAW pulse but occurs 50 ms later. No further electron movement is seen in the subsequent ten pulses.

In this device, rallies of over 60 pulses were possible with a single electron going back and forth between the quantum dots. A run of 35 transfers is shown in Fig. 2a, and the statistics of the full data set are shown in Fig. 2b. Rallies are broken when the transfer fails, which can occur in one of two ways. Occasionally, depopulation of the starting dot fails (marked F in Fig. 2b), in which case no electron arrives in the second dot. The chances of this can be reduced by increasing the potential of the starting dot, towards that of the channel, or by increasing the SAW amplitude, although larger SAWs can pose problems, for example by lifting the transferred electron over the barrier of the second dot. Given successful depopulation, transfer may still fail if the electron becomes trapped in the channel (marked T). This type of failure was more common in pulses from the weaker, right-hand, transducer and examples can be seen in Fig. 2a (also marked T). Here a SAW(R) pulse fails to transfer the electron all the way to the LQD, leaving it trapped in the channel. However, the next pulse from the other transducer recovers this electron, returning it to the RQD. The probability of recovery (marked R) is lower than the probability of transfer (marked S), indicating that electrons trapped in the channel may relax deeper into impurity traps than electrons that are carried through in SAW minima. This second type of error can also occur in another way (X, not shown), described later, but this can be eliminated by lowering the potential in the second dot.

A third error mechanism (marked E in Fig. 2b) is the arrival of an additional electron, which is then transferred with the initial electron. Electrons are seen to enter the system during pulses from the right-hand

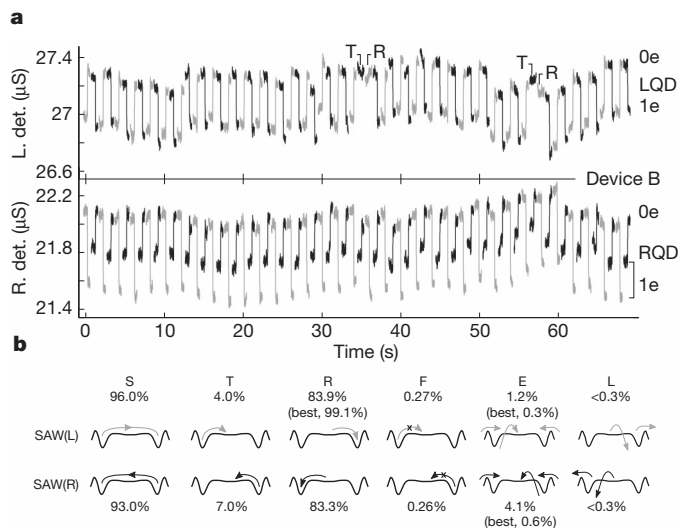


Figure 2 | Single-electron transfer reliability. **a**, Example of bidirectional electron transfer. An electron is transferred between the quantum dots 35 times before getting trapped in the channel (T). The next SAW(L) pulse recovers the electron (R). The SAW pulse duration is 300 ns, and the time between traces is not plotted. **b**, Transfer statistics for full data set (excerpt seen in **a**), showing probabilities of various events for SAW(L) and SAW(R): ideal transfer (S), depopulation to channel trap (T), recovery from channel (R), failure to depopulate (F), arrival of additional electron (E), loss of electron from system (L). Values in parentheses are for different voltages.

transducer that may have been caused or exacerbated by adjusting the RQD before the SAW(R) pulses started. No electrons appeared in the system during SAW(L) pulses. Increasing the isolation of the quantum dots and the channel from the surrounding reservoirs will reduce this. In none of the traces is the electron seen to leave the system (marked L).

The ability of SAWs to transport electrons depends on the SAW amplitude relative to the potential^{10,11}. Removing an electron from the starting dot requires a SAW of sufficient amplitude to overcome the sloping potential and lift the electron into the channel. If the SAW amplitude is too large, it will carry the electron over the far barrier and out of the second dot. Thus, there is a practical limit to the SAW amplitude for a given barrier–plunger combination, and for small-amplitude SAWs the dot needs to be raised towards the channel potential. Figure 3a shows the mean initial population of the LQD and Fig. 3b shows how depopulation changes with SAW power and plunger voltage (V_{LPG}). The potential gradient between the LQD and the channel decreases as V_{LPG} increases, allowing smaller-amplitude SAWs with a shallower gradient to lift electrons from the dot. Thus, the onset of depopulation occurs along a diagonal line, between the dashed lines in Fig. 3b, and depopulation of the deeper dots requires larger-amplitude SAWs.

The pulse width of the SAWs may be varied instead of the power. It has previously been shown¹² that a SAW can be used to modulate the barriers to an isolated dot, causing population and depopulation of the dot in a probabilistic process that requires many cycles to ensure a depopulation probability of $>50\%$. Figure 3c shows how SAW pulse width, that is, the number of attempts or SAW minima, affects depopulation of the LQD.

Applied pulses are not reproduced exactly in the SAW pulses owing to bandwidth limitations of the transducers; pulses longer than 14 ns should vary only in duration and not in peak amplitude. At a pulse width of 10.0 ns (27.7 cycles), the reduction in pulse amplitude due to transducer bandwidth is visible at the lower plunger voltages, where electrons cannot be depopulated. At 12.6 ns (34.9 cycles), just ~ 7 cycles more, depopulation is seen across almost the full range, and, as expected, at 14.5 ns the SAW is able to remove electrons over the same range as pulses of much longer width. From the rapid onset as the

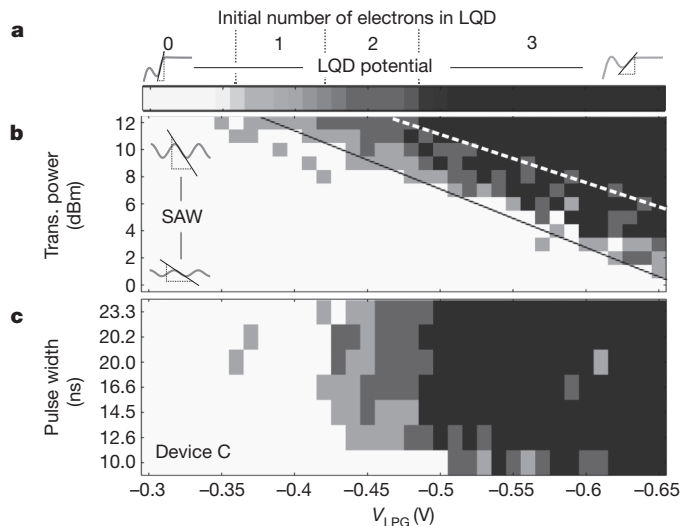


Figure 3 | Dependence of LQD depopulation on SAW power and pulse width. **a**, Initial population of LQD as a function of plunger voltage (V_{LPG}). The same greyscale key is used in **b** and **c** to indicate the number of electrons removed by the pulse. **b**, Depopulation of the LQD at different SAW(L) transducer powers; pulse width, 100 ns. The relative slope of the SAW (maximum slope as indicated) and the potential determine whether depopulation occurs. **c**, Depopulation of the LQD at different pulse widths for a SAW(L) power of 11 dBm. Pulse widths shorter than 14.5 ns do not achieve full amplitude, so depopulation fails at smaller values of V_{LPG} . By comparison with **b**, the peak SAW powers at pulse widths of 10 and 12.6 ns can be estimated as 7 and 10 dBm, respectively. Pulse widths are measured values of the microwave source and not linearly spaced.

pulse width increases, with depopulation going from approximately zero to complete in just 12.5 cycles, we can say that once a sufficient SAW amplitude is reached, depopulation occurs during the first few (~ 7) cycles of the pulse. Pulses applied to a transducer with a wider bandwidth (fewer fingers) would have shorter rise times, allowing this to be probed further.

This system also provides a method of investigating energy loss mechanisms for electrons above the Fermi energy. As a SAW minimum transfers an electron, it lifts it over 'bumps' in the potential, raising and lowering its potential energy as necessary. However, when the potential gradient exceeds the maximum SAW gradient, confinement is lost and a 'hot' electron escapes backwards towards the channel (Fig. 4a). The energy at which this occurs depends on the underlying potential. Figure 4b shows how varying the right-hand barrier voltage (V_{RBG}) affects the escape probability and the initial energy of escaping electrons. An electron starts in the RQD and a long (300-ns) SAW pulse is sent from the left. Electrons escaping the SAW potential at a low energy will remain in the dot (Z in Fig. 4a), at higher energies they will escape to the channel (Y), and at energies above the channel maximum they will reach the LQD (X). During a pulse, an X or Y electron may be returned to the RQD and 'recycled', with its ultimate position (LQD, trapped in channel, RQD) being determined during the last part of the SAW pulse as the amplitude drops. For $V_{RBG} > -1.2$ V, transfer to the LQD is unlikely, no electrons are transferred to the LQD and the probability of staying in the RQD (Z) is $>90\%$. For $V_{RBG} < -1.3$ V, the probability of leaving the RQD (X or Y) increases to $>50\%$ and the probability of escaping to the LQD (X) reaches 25%. In Fig. 4b, open symbols are for a less negative plunger voltage and show a reduced probability of transfer from the RQD because this dot is correspondingly deeper.

Electrons with a large excess of energy rapidly lose energy by emitting an optical phonon (of energy 36 meV) in about 1 ps (ref. 13), comparable to the time taken by an electron to cross one quantum dot. Electrons with energies less than 36 meV can emit acoustic phonons only with typical energies ≤ 0.1 meV, and emit these phonons more slowly. In the low-energy limit, this is on a 100-ns timescale¹⁴. The addition of a gate across the centre of the channel, capable of being

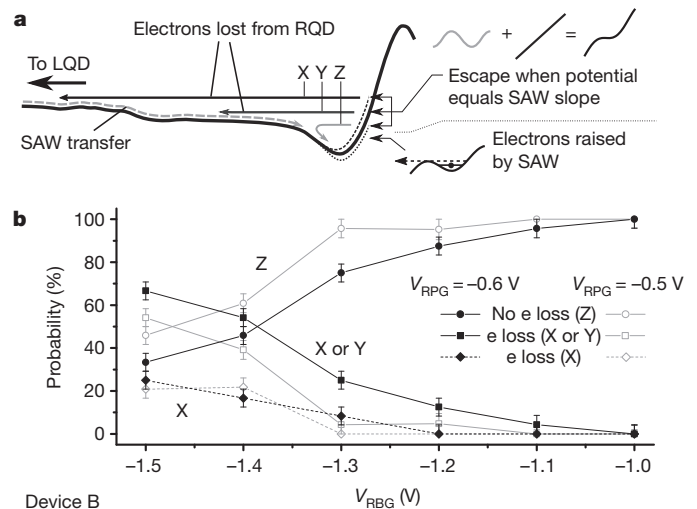


Figure 4 | Backscattering of electrons in the RQD due to SAW(L). **a**, An electron in the RQD will be lifted up the right-hand barrier by SAW(L) until it either leaves the system or the underlying potential becomes too steep for the SAW minimum to retain the electron. Electrons remain in the dot (Z), escape to traps in the channel (Y) or escape to the LQD (X). **b**, Probabilities of events X, Y, Z, and Z as functions of barrier voltage. (Open symbols are for a slightly deeper RQD potential (V_{RPG})). A threshold is evident at around -1.3 V: for $V_{RBG} < -1.3$ V, escape to the LQD is possible, whereas for $V_{RBG} > -1.3$ V, escape to the LQD is prevented by the channel potential. Error bars, 1 s.d.

pulsed at high frequencies, would provide a method of investigating emission of acoustic phonons by high-energy electrons.

This source of high-energy electrons may be of use in p-n junction devices as a way to controllably introduce single electrons into a region of holes as a single-photon source¹⁵, without requiring negatively charged gates in close proximity to the holes.

To be useful in a quantum information circuit, the transfer of an electron must not cause its spin state to decohere. Coherent transfer of a collection of spins has been demonstrated over a distance of 70 μm (for a particular wafer orientation), with the potential to extend this much further¹⁶; and coherent oscillations of charge have been shown over a submicrometre distance¹⁷. Fluctuations in the magnetic field created by nuclear spins (B_{Nuc}) are the main cause of dephasing in static quantum dots; however, an electron trapped in a moving SAW quantum dot samples many different local B_{Nuc} fields, spending only a brief time in each. The average B_{Nuc} , and hence, dephasing, is reduced by three orders of magnitude owing to the motion of the SAW (more details of dephasing mechanisms are given in Supplementary Information). It is therefore likely that coherent transfer of spins is achievable and that dephasing will actually be suppressed during transfer.

In an ideal quantum dot network, with a perfectly smooth potential, an electron could simply be allowed to 'roll' from an elevated starting dot down to the second dot. In practice, the potential is far from perfect and irregularities in the background potential would make this method of transfer highly unreliable. A pulse of SAWs, however, can be used to modulate the channel temporarily, assisting the transfer in a peristaltic-like movement, the amplitude of which can be tuned to the minimum required to overcome desired obstacles, allowing on-demand removal and delivery of single electrons between distant quantum dots in a manner that should be compatible with many of the quantum computing proposals based on electronic spin states in semiconductors.

METHODS SUMMARY

The two-dimensional electron gas was formed at the interface of a GaAs/AlGaAs heterostructure. Before depletion, the carrier density was $1.6 \times 10^{11} \text{ cm}^{-2}$ and the carrier mobility was $1.8 \times 10^6 \text{ cm}^2 \text{ V}^{-1} \text{ s}^{-1}$. We made several devices; results for devices B and C are reported here. Devices and transducers were patterned by electron-beam lithography. All measurements were made at 300 mK. Radio-frequency signals were applied to transducers using an Agilent 8648D source

(external modulation option). To prevent Bragg reflections, transducers were of double-element design¹⁸, with 30 pairs of fingers. The detector circuits shared a common source with a ~ 1 -mV d.c. bias. In device B, the position of the RQD was adjusted between the capture and transfer positions to aid depopulation by the weaker, right-hand, transducer. This adjustment shifted the dot minimum relative to the right-hand detector, making the return steps smaller. The gate set-up time between traces was 2–8 s. The applied radio-frequency power in Fig. 1d was 10 dBm for SAW(L) and 18 dBm for SAW(R), and the attenuation from the source to the transducers was 10 dB for SAW(L) and 20–30 dB for SAW(R).

Received 5 May; accepted 12 August 2011.

1. Loss, D. & DiVincenzo, D. P. Quantum computation with quantum dots. *Phys. Rev. A* **57**, 120–126 (1998).
2. Barnes, C. H. W., Shilton, J. M. & Robinson, A. M. Quantum computation using electrons trapped by surface acoustic waves. *Phys. Rev. B* **62**, 8410–8419 (2000).
3. Petta, J. R. *et al.* Coherent manipulation of coupled electron spins in semiconductor quantum dots. *Science* **309**, 2180–2184 (2005).
4. Pioro-Ladrière, M. *et al.* Electrically driven single-electron spin resonance in a slanting Zeeman field. *Nature Phys.* **4**, 776–779 (2008).
5. Elzerman, J. M. *et al.* Single-shot read-out of an individual electron spin in a quantum dot. *Nature* **430**, 431–435 (2004).
6. Hanson, R. *et al.* Single-shot readout of electron spin states in a quantum dot using spin-dependent tunnel rates. *Phys. Rev. Lett.* **94**, 196802 (2005).
7. Morello, A. *et al.* Single-shot readout of an electron spin in silicon. *Nature* **467**, 687–691 (2010).
8. Hanson, R., Kouwenhoven, L. P., Petta, J. R., Tarucha, S. & Vandersypen, L. M. K. Spins in few-electron quantum dots. *Rev. Mod. Phys.* **79**, 1217–1265 (2007).
9. Field, M. *et al.* Measurements of Coulomb blockade with a noninvasive voltage probe. *Phys. Rev. Lett.* **70**, 1311–1314 (1993).
10. Kataoka, M., Barnes, C. H. W., Beere, H. E., Ritchie, D. A. & Pepper, M. Experimental investigation of the surface acoustic wave electron capture mechanism. *Phys. Rev. B* **74**, 085302 (2006).
11. Rahman, S., Kataoka, M., Barnes, C. H. W. & Langtangen, H. P. Numerical investigation of a piezoelectric surface acoustic wave interaction with a one-dimensional channel. *Phys. Rev. B* **74**, 035308 (2006).
12. Kataoka, M. *et al.* Single-electron population and depopulation of an isolated quantum dot using a surface-acoustic-wave pulse. *Phys. Rev. Lett.* **98**, 046801 (2007).
13. Taubert, D. *et al.* Relaxation of hot electrons in a degenerate two-dimensional electron system: transition to one-dimensional scattering. *Phys. Rev. B* **83**, 235404 (2011).
14. Fujisawa, T. *et al.* Spontaneous emission spectrum in double quantum dot devices. *Science* **282**, 932–935 (1998).
15. Gell, J. R. *et al.* Surface-acoustic-wave-driven luminescence from a lateral p–n junction. *Appl. Phys. Lett.* **89**, 243505 (2006).
16. Stotz, J. A. H., Hey, R., Santos, P. V. & Ploog, K. H. Coherent spin transport through dynamic quantum dots. *Nature Mater.* **4**, 585–588 (2005).
17. Kataoka, M. *et al.* Coherent time evolution of a single-electron wave function. *Phys. Rev. Lett.* **102**, 156801 (2009).
18. Morgan, D. *Surface Acoustic Wave Design* 9–18 (Academic, 2007).

Supplementary Information is linked to the online version of the paper at www.nature.com/nature.

Acknowledgements The authors acknowledge funding from the UK EPSRC, Toshiba Research Europe Limited and QIPIRC.

Author Contributions R.P.G.M., M.K., C.J.B.F. and C.H.W.B. designed the experiment; I.F. and D.A.R. provided wafers; D.A. and G.A.C.J. performed electron-beam lithography; R.P.G.M. processed samples and analysed data; R.P.G.M. and M.K. performed experiments; R.P.G.M., C.J.B.F. and M.K. wrote the paper.

Author Information Reprints and permissions information is available at www.nature.com/reprints. The authors declare no competing financial interests. Readers are welcome to comment on the online version of this article at www.nature.com/nature. Correspondence and requests for materials should be addressed to C.J.B.F. (cjbf@cam.ac.uk).